D. Leutloff, R.C. Srivastava (Eds.)
Computational Fluid Dynamics: Selected Topics,
Springer, 1995, pp. 219-232

Inertial convection in turbulent Rayleigh-Bénard convection at small Prandtl numbers

Dedicated to Prof. K.G. Roesner, TH Darmstadt
to his 60-th birthday

G.Grötzbach, M. Wörner
Kernforschungszentrum Karlsruhe, Institut für Reaktorsicherheit,
Postfach 3640, D-76021 Karlsruhe

Abstract. Inertial convection is a two-dimensional flow mechanism effectively transporting heat. It was predicted theoretically to exist in Rayleigh-Bénard convection in liquid metals at Rayleigh numbers above 10^4. In numerical simulations it was found in this range and at smaller Rayleigh numbers. Here, the method of direct numerical simulation is used to study the details of inertial convection in the fully turbulent regime in liquid sodium, Pr = 0.006, at Ra = 24,000. Application of a semi-implicit time integration scheme and of a fast elliptic solver make such simulations possible. The results show the inertial convection still exists in this range of Ra, but it occurs only locally and over certain time intervals in that areas in which the flow is roughly two-dimensional at large scales. In an aperiodic oscillation this flow mechanism is in competition to a more irregular, three-dimensional flow state. The Nusselt numbers at both walls oscillate with the changing flow structure. They show larger values during the occurrence of the inertial convection and smaller ones with the irregular flow.

Introduction

In new designs of liquid metal cooled nuclear reactors the removal of decay heat in accident situations is achieved by pure natural convection. Experiments are performed in scaled reactor models with water to analyse the corresponding flow phenomena and temperature transients [1]. The interpretation of the experiments and the transfer of the results to real reactor conditions is mainly done by computer codes [1,2]. The turbulence models used in such codes have to be adapted to be applicable to purely buoyant flows and to liquid metals. One effort in this context is to determine turbulence data in simple flows to calibrate existing models, e.g. from experiments with jets [3] and heated spheres [4], or from direct numerical simulations for Rayleigh-Bénard convection [5,6]. From those simulation results it is deduced that common transport equation models are incomplete in a sense that terms are neglected which turn out to be dominant in pure natural convection. For some of the missing terms no models are known. Therefore, a complementary effort is to gain a better un-

derstanding of the physical mechanisms in natural convection of liquid metals to form a basis for the development of improved turbulence models.

Rayleigh-Bénard convection is the upward directed convective heat transfer through a large horizontal fluid layer enclosed between two plane walls. For common fluids with Prandtl numbers $Pr = \nu/\kappa$ (ν = viscous diffusivity, κ = thermal diffusivity) around one the flow development and the mechanisms are well known [7]. The flow develops from no motion at small heating rates, that is at small Rayleigh numbers ($Ra < Ra_{cr} = 1{,}708$, with $Ra = g\,\beta\,\Delta T_w\,D^3/(\nu/\kappa)$, g = gravity, β = volume expansion coefficient, ΔT_w = temperature difference between both walls, D = distance between walls), through steady two-dimensional and three-dimensional flows, through time-dependent three-dimensional flows, to a fully turbulent flow at large heating rates. Some uncertainty exists regarding the turbulent regime. This was subdivided in a regime with soft and hard turbulence, each one showing its own statistical features [8], but recent simulation results showed that the differences between hard and soft turbulence occur only as a consequence of different aspect ratios of the channels used [9]. Rayleigh-Bénard convection is per definition the heat transfer through an infinite horizontal fluid layer, and therefore a kind of hard turbulence found at small aspect ratios is not a separate flow status of this flow.

Liquid metals have very small Prandtl numbers; their thermal diffusivity is much larger than their viscous diffusivity. Therefore, the heat transfer by molecular conduction is dominant up to much larger heating rates than in fluids with small thermal diffusivity. The transition from no motion to irregular flow extends in experiments only over a range of Rayleigh numbers being apart less than a factor of two [7]. This very different behaviour was also predicted theoretically [10]. Thus one finds in liquid metals already at small Ra very irregular or turbulent convection, but the heat transfer rate only shows considerable convective contributions at much larger Ra ($Ra > 10^4$), see e.g. the experiments of [11,12]. In this range a fly-wheel type of convection, called inertial convection, is predicted by two-dimensional methods to occur [13], but experimentally indications for the inertial convection are found even at smaller Rayleigh numbers [14]. With three-dimensional simulations of Rayleigh-Bénard convection in liquid sodium, which gave the first field data on the velocity field in this type of flow, we could show that inertial convection definitely exists at $Ra = 3{,}000$ and 6,000 and that the flow becomes more irregular with increasing Rayleigh number [6,15]. Indicators for the inertial convection seem to be small secondary vortices near the walls between the larger rolls and a more regular, roughly two-dimensional arrangement of the rolls.

In this paper we use the method of direct numerical simulation to analyse Rayleigh-Bénard convection in liquid sodium, $Pr = 0.006$, at a Rayleigh number of 24,000. The simulation model TURBIT [16] had to be extended by a semi-implicit time-integration scheme for the energy equation to allow for these simulations [6,17]. The simulation results are analysed regarding the large scale features of the flow, especially regarding the existence of the inertial convection when three-dimensional methods are used in this range of Rayleigh numbers, and regarding the dynamics of the flow. The mechanisms of the spe-

cial flow features found are explained and their influences on the heat transfer capabilities are investigated.

Simulation Method

The simulation model used is the TURBIT code [16]. It is based on the complete three-dimensional time-dependent conservation equations for mass, momentum, and energy for a Newtonian fluid. The fluid is considered to be incompressible; for the buoyancy term the validity of the Boussinesq approximation is assumed. The equations are made dimensionless by the length scale D, by the velocity scale $(g\,\beta\,\Delta T\,D)^{1/2}$, and by the temperature scale $\Delta T = T_{w1} - T_{w2}$. The code uses a finite volume scheme on a staggered grid. The pressure is calculated by Chorin's projection method. The resulting Poisson equation can be solved efficiently in simple geometries like in infinite plane channels by direct methods [18].

The time integration scheme used originally in the code is the second order explicit Euler-leapfrog scheme. Application of this scheme to natural convection in liquid metals leads to enormous CPU-time requirements. The stability criterion of this explicit scheme can be written by using Einstein's summation convention [19]:

$$\Delta t \leq \left(\frac{|u_i|_{max}}{\Delta x_i} + 4\,\frac{Max\,(\nu, \kappa)}{\Delta x_i^2} \right)^{-1}, \qquad (1)$$

where u_i, $i = 1, 2, 3$, denotes the components of the velocity vector and Δx_i denotes the grid widths. The temperature field in natural convection of liquid metals is governed by the large thermal conductivity allowing only for large scale structures in the temperature field and for thick thermal boundary layers. In contrast, the velocity field has not only large scales but also very small spatial structures and very thin viscous boundary layers near walls. For direct numerical simulations of turbulence it is essential to choose grids which resolve all relevant length scales of the flow. Therefore, the velocity field requires very fine grid widths. Thus, the diffusion terms become dominant in the stability criterion (1) and liquid metals require very small time steps for numerical stability of the thermal diffusion. These time steps are much smaller than those required to ensure stability of even the highest frequencies in the convective time scales. Substantially larger time steps can be achieved by time integration schemes which do not have the thermal diffusivity in the stability criterion. Thus, the diffusive terms of the energy equation have to be treated implicitly, whereas all other terms may still be treated explicitly.

Recently the code was extended by two semi-implicit time integration schemes [6,17] which can be used alternatively. They were selected to be suit-

able for diffusion dominated problems and to be consistent with the explicit scheme used for the velocity field. Both semi-implicit schemes treat the diffusive terms $L = \kappa \nabla^2 T$ by the implicit Crank-Nicolson method, CN, whereas for the non-linear convective terms $N = \underline{u} \nabla T$ the explicit Adams-Bashforth, AB, eq. (2), or the Leapfrog scheme, LF, eq. (3), is used, respectively:

$$\frac{T^{n+1} - T^n}{\Delta t} = \frac{1}{2}\left(3\, N^n - N^{n-1} \right) + \frac{1}{2}\left(3\, L^{n+1} + L^n \right). \quad (2)$$

$$\frac{T^{n+1} - T^{n-1}}{2\Delta t} = - N^n + \frac{1}{2}\left(L^{n+1} + L^{n-1} \right). \quad (3)$$

Here n denotes the time level. In the code both schemes are realized in a way that, like the fully explicit scheme, both are started by an Euler step, and after about 40 to 60 time steps an averaging step is used to damp spurious oscillations which might develop in the solution.

A von Neumann stability analysis for the linearized problem indicates the LFCN scheme should be stable for Courant numbers $C = u_{max}\, \Delta t / \Delta x_{min} < 1$ and for any value of the diffusion number $D = \kappa\, \Delta t / (\Delta x_{min}^2)$, whereas the stability criterion of the ABCN scheme depends on the diffusion number and always needs some diffusion for stability. Practical tests showed that both schemes become unstable in some applications for diffusion numbers of about six and greater. To avoid these stability problems a maximum value for the diffusion number was chosen, $D_{max} = 4$. This gives an upper limit for the time step width calculated from eq. (1) with $\kappa = 0$.

The sets of linear equations resulting from the implicitly treated diffusion terms are those from a Helmholtz equation. Thus, in principle these sets can be solved with general Helmholtz (or most Poisson) solvers. With direct numerical simulations, the coefficients of the Helmholtz equation are space dependent, but their space dependence can be separated; therefore very efficient direct Poisson solvers, like from [18], can be used. More serious difficulties are due to the manifold of combinations of wall conditions used in the thermal diffusion term (von Neumann and/ or Dirichlet conditions), which are usually not all available with common fast solvers. Correspondingly, the boundary conditions of the package from [18] were extended. As a result of using modified direct Poisson solvers to solve the set of equations resulting from the semi-implicit time integration scheme, the additional CPU-time is only 10 - 20 % of that of the fully explicit scheme. The storage requirement is about the same as that of the fully explicit scheme. As the time step can be increased, e.g. for sodium at least by one order of magnitude, this method provides the efficiency required to make these simulations possible.

Case Specifications and Initial Data

For simulation of Rayleigh-Bénard convection a plane channel should be considered which is infinite in both horizontal directions. This is achieved in the simulation by using periodic boundary conditions in both horizontal directions. The periodicity lengths are X_i, with i=1,2, Fig.1. They have to be chosen large enough to resolve all large scale phenomena. In earlier simulations for common fluids with Prandtl numbers around Pr = 1 these lengths turned out to have a strong influence on the heat transfer through the fluid layer [9,20]. Even our recent simulations with X_i/D = 7.92 [15,21] seem not to fulfil all requirements of a complete statistical decoupling in the horizontal directions. In liquid metals the large thermal diffusivity is responsible for an even farer horizontal coupling and therefore for larger scales, but there are no data available from experiments to select adequate periodicity lengths. From simulations on a coarse grid for Ra = 6,000 using horizontal extensions X_i/D from 4 to 16 we found, that the large scale features of the flow simulated for aspect ratios of 8 and greater are almost independent on the aspect ratio [6]. Therefore we used X_i = 8 for the convection in sodium also at the Rayleigh number considered here, Ra = 24,000, which is in the fully turbulent regime.

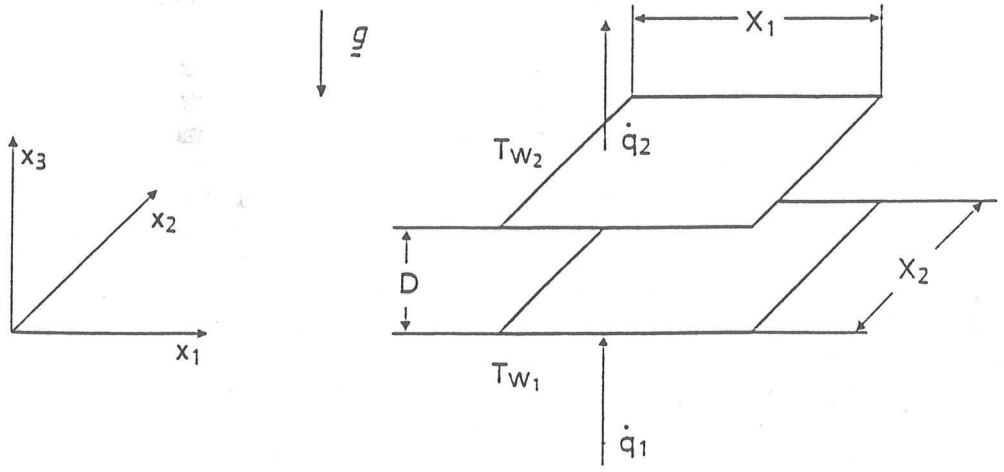

Fig.1: Geometry and definitions for the Rayleigh-Bénard problem.

In direct numerical simulations not only the large scales have to be resolved adequately, but also the small scales. The smallest scales in liquid metals occur in the velocity field. The size of these can be calculated on several ways [20], e.g. by means of the Kolmogorov length scale and by the Grashof analogy [22]. The latter means the statistical features of the small scales in the velocity field were found to be similar in different fluids for comparable Grashof numbers, Gr = Ra / Pr, and therefore the mean dissipation profile needed to calculate the Kolmogorov length is similar. The profile can be taken from simulations or experiments for other fluids. The finest grids using $N_1 = N_2$ = 250 mesh cells

in each horizontal direction, Tab. 1, are finer than the Kolmogorov scale at any position in the channel.

Tab.1: Case specifications and simulation times on a SIEMENS/FUJITSU VP400-EX. Each case is started from that one on the line above.

Ra	Gr	$N_1 = N_2$	N_3	Δx_{3w}	t_{max}	N_t	CPU/ VP400
12,000	$2*10^6$	128	19	0.03	358.8	16,000	
12,000	$2*10^6$	160	25	0.02	400.1	19,040	
12,000	$2*10^6$	160	31	0.01	410.1	22,000	
12,000	$2*10^6$	200	35	0.008	411.5	22,640	
12,000	$2*10^6$	250	39	0.005	444.4	61,440	55 h
24,000	$4*10^6$	250	39	0.005	471.5	84,000	60 h

Linear wall approximations are applied for the diffusive terms in the mesh cells next to the walls. Therefore, the viscous and thermal boundary layers have to be resolved sufficiently by the grid. In liquid metals the viscous layer is the finer one. The Grashof analogy is used to specify the vertical resolution by the vertical grid width Δx_{3w} near the wall. The criterion of [20] to use at least 2 to 3 cells inside the boundary layer is sufficient from an engineering point of view, e.g. to get sufficient accuracy in the global energy balance or in the Nusselt number, but in studying terms from turbulence models based on second order transport equations, a much finer resolution is required near the walls for analysing purposes. In using a non-equidistant vertical distribution the number of vertical nodes can be limited to $N_3 = 39$, Tab.1.

Initial conditions are gained from the last run of a series of simulations for Ra = 12,000, Tab. 1. The first case used a coarse grid, zero velocities, and random temperature fluctuations superimposed to a schematic piecewise linear vertical profile of the mean temperature which roughly represents a realistic initial vertical mean energy distribution. The other simulations on the finer grids for Ra = 12,000 are started from the simulation results for the same Rayleigh number gained from the next coarser grid using parabolic spatial interpolation.The interpolated data on the fine grid show increased fluctuation amplitudes at small scales, Fig. 2, but after integration over a time period between 0.1 and 1 dimensionless time units the spectrum is as steep again as the theoretically expected k_1^{-7} slope. For Ra = 24,000 the simulation results for the smaller Rayleigh number on the finest grid are used as initial data; this is possible without any transformation of the data because with the scaling, especially of the velocities, chosen here the dimensionless velocity values do not change

with Ra at large Rayleigh numbers. Both latter methods of creating initial conditions turned out to allow for reductions of CPU-times by one order of magnitude or more compared to runs starting from more or less random data on the required fine grid. The CPU-times given in Table 1 are those on the finest grids only. The number of time steps N_t is consecutively counted through the complete sequence of runs.

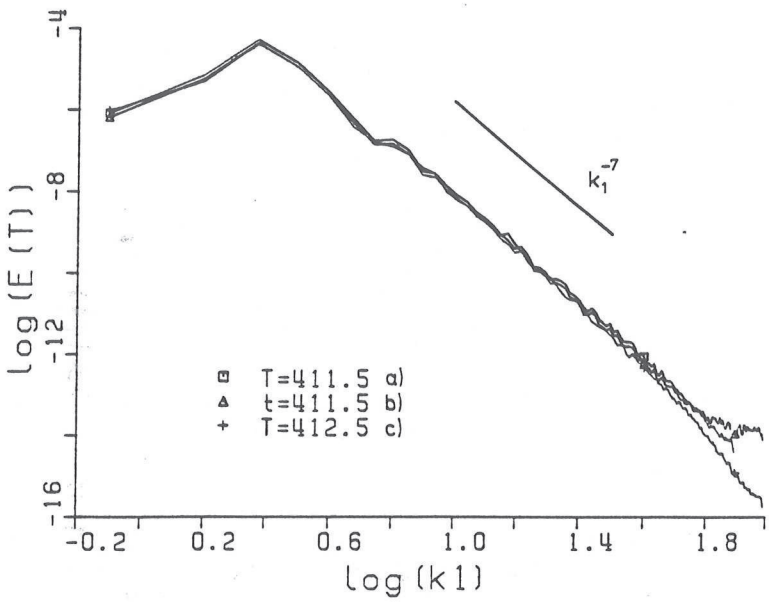

Fig.2: One-dimensional energy spectra of temperature fluctuations over wave number k_1 at channel mid plane, $x_3=0.5$, for Ra = 12,000, a) coarse grid, 200^2*35, t=411.5, b) same result interpolated to fine grid, 250^2*39, c) fine grid, 250^2*39, after integration to t=412.5.

RESULTS

Verification

Problems in verifying these simulation results occur due to the complete lack of detailed turbulence data on the velocity field in Rayleigh-Bénard convection of liquid metals and due to the existence of only very few data on the temperature fields. In [6,23] all available data are used to perform a verification. As the uncertainties of the experimental results are rather large, additional recalculations of experiments for air [22] and the recalculation of GAMM benchmarks [17] were used to verify the implementation of the semi-implicit time integration scheme.

A very crude verification, especially of the periodicity lengths chosen, can be deduced from horizontal cuts through the instantaneous temperature

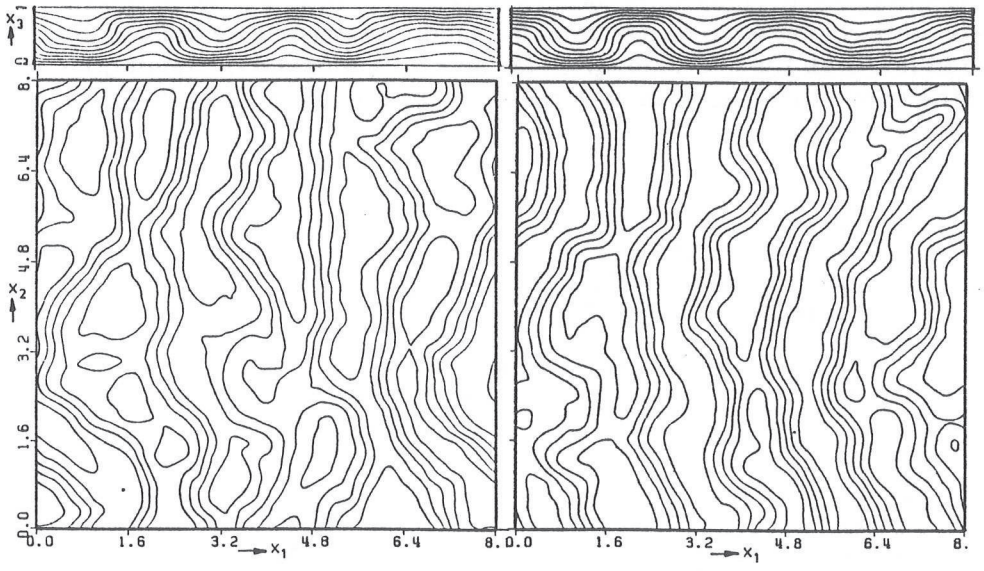

Fig.3: Contourlines of instantaneous temperature fields at Ra = 24,000; isoline increment 0.1, top vertical cuts at $x_2=6.816$, bottom horizontal cuts at $x_3=0.5$, left $t=478.7$, right $t=488.3$.

fields, Fig.3. Despite a fully turbulent state these figures show band-like structures. According to [24] this indicates the existence of remainders of regular vortex systems. The wavelength of this structure is about 2.7. This is, as to be expected, above the value at the critical Rayleigh number [10] and it shows that the periodicity lengths chosen can represent about 3 vortex pairs. This resolution for large scale structures is better than in other published simulations for other fluids, e.g. in [9,25]. From the vertical cuts it gets obvious that convection only weakly contributes to the heat transfer. Accordingly, the Nusselt number analysed is with 1.36 near one. This is in reasonable agreement with experiments [11,12].

Flow Mechanisms and Dynamics

According to current knowledge the Rayleigh number Ra = 24,000 of this simulation is in the turbulent regime. Nevertheless the instantaneous temperature fields at both times give large band-like structures which indicate the existence of irregular roll systems, Fig.3. Vortex bands are indeed found in the velocity field, for example in u_3, Fig.4. There exist three large vortex pairs which are locally disturbed in a three-dimensional manner. In the simulations for smaller Ra it was found that the inertial convection coexists with small secondary currents near the walls [6,24]; here those parts of the secondary currents which have positive vertical velocities are found as small clouds in the down-

draft area. Thus, there are indicators for the existence of remainders of the inertial convection. Indeed, the analysis of a time sequence of such figures in the form of a computer generated movie shows there is always a competition between the formation of two-dimensional structures, which are necessary to form inertial convection [13], and their destruction by meandering into more irregular, three-dimensional ones.

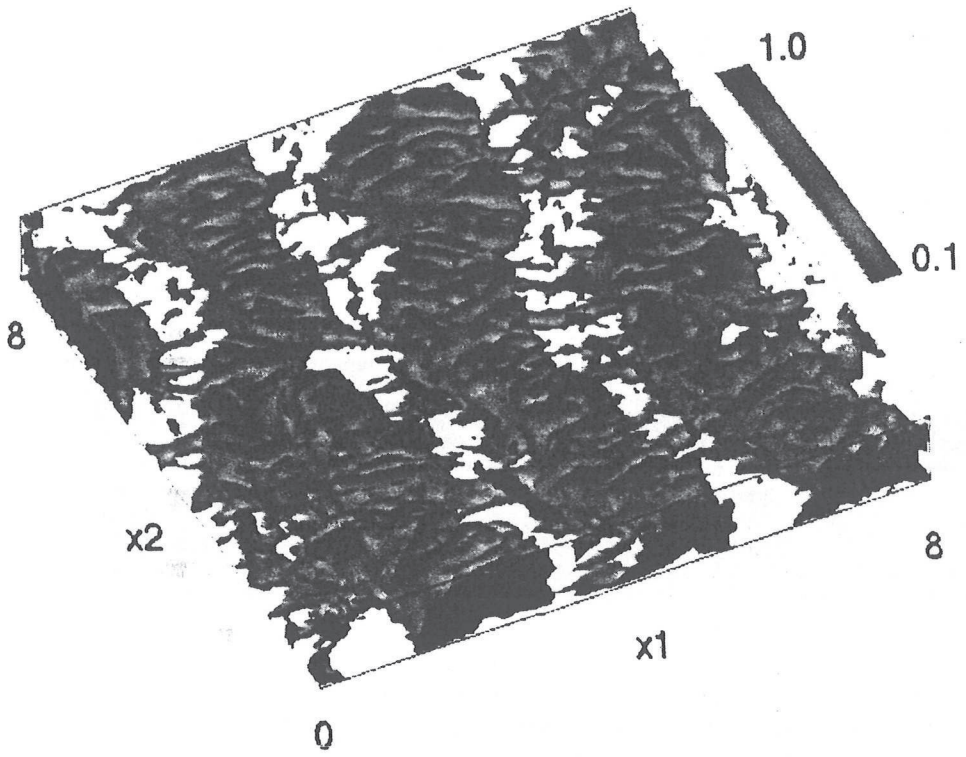

Fig.4: Isosurface for a small positive value of the vertical velocity, $u_3=0.05$, colour code for the temperature. Ra = 24,000, t=488.3. Inside the isosurface the flow is upward, outside it is mainly downward.

A more detailed search for the inertial convection is performed in that areas and at that times in which a pronounced two-dimensional character of the flow field is found. Scanning through the velocity data for t = 488.3 shows nearly everywhere a highly irregular, turbulent flow field, Fig. 5. However, only near $\{x_1=2, x_2=6.8\}$ one pair of vortices is found that shows an arrangement in the channel which is symmetrical to the mid plane and that has a regular radial velocity distribution. It extends from about $x_1 = 1.2$ to about $x_1 = 3$, and in the axial direction it has a length between one and two D. The life time is only a few time units. The corresponding profile for the vertical velocity component in that plane confirms, this vortex pair has a velocity profile which is linear over a larger area. That means, each of these vortices rotates at least in the inner part like a solid body. Outside the range of these two vortices, that is below $x_1 = 1.5$

and above $x_1 = 2.5$, the velocity profile is highly irregular or turbulent, as it is to be found in all other parts of the channel.

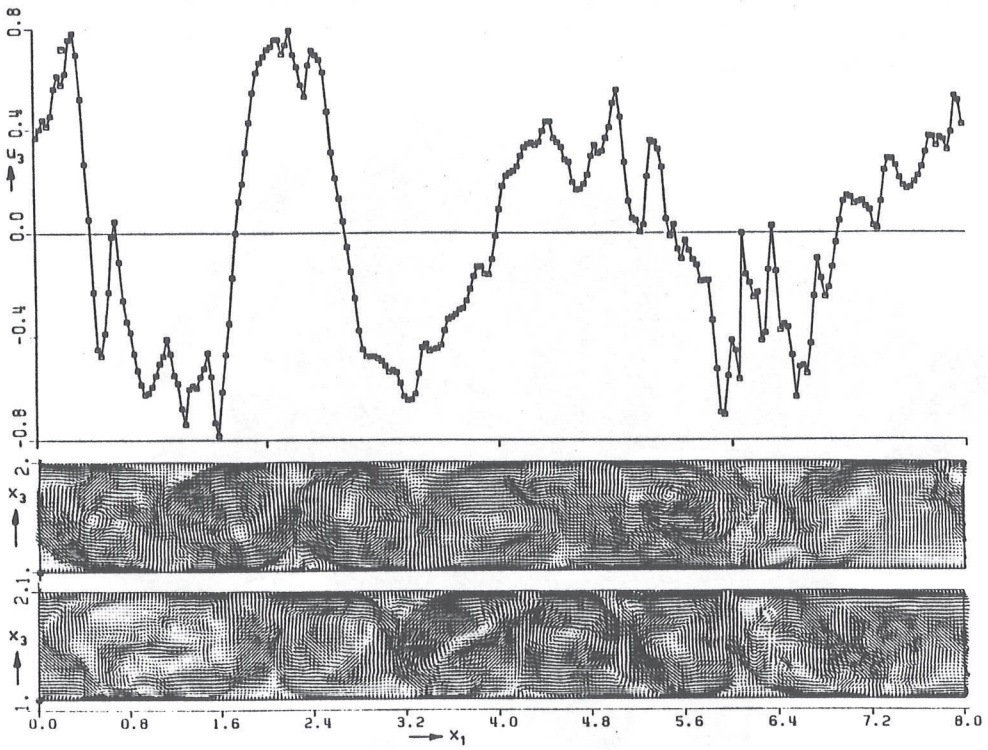

Fig.5: Instantaneous profile of vertical velocity u_3 at $\{x_2=6.81, x_3=0.5, t=488.3\}$,top, and vector plots for $\{u_1,u_3\}$ at $\{x_2=6.81, t=488.3\}$, middle, and at $\{x_2=2.81, t=488.3\}$, bottom.

The corresponding temperature field shows in the horizontal sections wide areas with roughly two-dimensional character, that is not only in the area around $\{x_1=2, x_2=6.8\}$, but also in a much larger surrounding, Fig. 3. In the vertical sections one finds according to the small value of the Nusselt number only slight distortions by convection, except for $t=488.3$ in that area in which the inertial convection was found in the velocity field. There we find stronger distortions of the isolines toward the upper wall in the centre of the vortex pair and towards the lower wall in both outer areas of the vortex pair. This means the inertial convection is locally and for short times responsible for an intensive vertical heat transfer by convection.

With these results the aperiodic production and destruction of the inertial convection can be explained like follows: Vortices rotating like solid bodies obey no internal dissipation. Therefore, the rotation speed grows to large values, and thus also the convective heat transfer is augmented. Increasing rotation speeds lead to shear instabilities near the walls and therefore to irregular,

three-dimensional structures. These are more dissipative and do not allow for such large velocities. The rotation speed is decreasing and the convective heat transfer is reduced. The molecular heat transfer becomes dominant. It filters off the small scale fluctuations produced by the irregular, turbulent flow. Thus, the flow relaminarizes locally and starts to form regular rolls again.

Considering the small scales of the velocity field, an other phenomenon is found in liquid metals. Thin spoke pattern like structures exist extending across the rolls, Fig. 4. These spoke patterns were not observed at the Rayleigh numbers 3,000 and 6,000 analysed earlier [6, 24]. They do not only exist near the lower wall, but also near the upper wall as is indicated by a very rugged isosurface. These structures are formed by thin bands with upward moving fluid in the downdraft area near the lower wall and by downward moving fluid in the updraft area near the upper wall. The spoke patterns show the flow is highly three-dimensional at small scales. The patterns found here for sodium are comparable to the spoke-pattern like structures found at the edge of the viscous boundary layer in several direct simulations for air at comparable Grashof numbers [21,24,25]. In general, the velocity field at this Rayleigh number obeys much smaller scales as the temperature field and correspondingly it has also smaller time scales.

A statistical analysis at midplane shows that the flatness of the vertical velocity component is near 3, which indicates Gaussian distributions and therefore turbulent features, whereas the flatness for the temperature field is around 1.7. Thus, it is nearer to 1.5, which is the value for a sinusoidal distribution. This means, the band-like structures are still dominant in the temperature field, despite they can be identified in the contourline presentations of horizontal cuts through the temperature field, Fig.3, only over short times and only locally.

Heat Transfer Statistics

The integral heat transfer capabilities are analysed by means of a time history for plane averaged Nusselt numbers at both walls, Fig.6. As these data are not time-averaged, the consequences of the irregular oscillations found in the flow become obvious. The Nusselt numbers change within a 10%-band. The corresponding oscillations are very slow. Therefore, immense averaging times are required in experiments to determine accurate results for the Nusselt numbers.

Correlating the time-dependent Nusselt numbers to the instantaneous temperature fields, Fig.3, shows the wall heat fluxes always reach a larger value at those times at which the flow field is more regular or two-dimensional. They are large especially in those time intervals in which the inertial convection occurs; compare the times used in Fig. 3 and 5. The Nusselt numbers exhibit smaller values at times with more irregular or three-dimensional flow fields. From Fig. 5 it can be deduced that the inertial convection is a flow with rather large rotation velocities and that it occurs only over short times extending over small parts of the channel. This means the inertial convection is a type of flow which

has a strong influence on the overall heat transfer in the channel. It maximises the convective heat transfer.

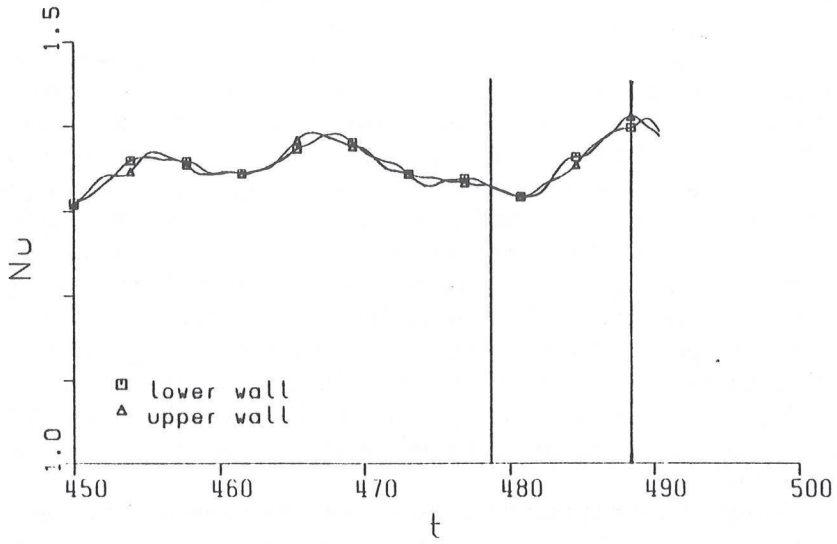

Fig.6: Time dependent Nusselt numbers at lower and upper walls averaged horizontally. Ra = 24,000. The vertical lines mark the times for which the temperature fields are given in Fig.3.

CONCLUSIONS

The method of direct numerical simulation is used to investigate Rayleigh-Bénard convection in liquid metals. The large thermal conductivity of these fluids requires an implicit treatment of the thermal diffusion term. This, and using extended direct Helmholtz solvers, ensures efficient simulations and make such simulations possible at all. The long time periods to be simulated need additional measures like using not too fine grids for the development phase of the flow and interpolation of results from coarser grids to finer grids, on which the final time interval is simulated which is finally used for analysis.

The inertial convection was predicted by theoretical two-dimensional methods to occur in Rayleigh-Bénard convection of liquid metals at Rayleigh numbers above 10^4. With former direct simulation results it was shown that in the expected range of Ra indications for this flow mechanism, like a locally two-dimensional flow field and small secondary currents, are found, but that pronounced forms of inertial convection exist only at smaller Rayleigh numbers. This is in agreement with indications from experiments. Simulation results for Ra = 24,000 are analysed here in more detail regarding the instantaneous local velocity distributions. Small areas are found in the channel only for short times in which large scale vortex pairs exist which rotate like a solid body. These vorti-

ces are found only in small parts of those regions in which the flow is roughly two-dimensional and in which small counter rotating secondary vortices occur near the walls. This means, local two-dimensionality and secondary vortices are no sufficient indicators for the inertial convection because these indicators occur also outside those areas. The velocity field also shows the inertial convection at these Ra is superimposed by highly three-dimensional spoke patterns. These patterns consist of small and fast scales which clearly show the highly turbulent nature of these flows. Thus, with increasing Rayleigh number the inertial convection does not vanish abruptly, but it is still occurring locally and for short time periods. It is in competition to three-dimensional flow structures and forms an aperiodic oscillation. Large computational domains are required to find such changes in flow structures. In analysing the integral heat transfer through the fluid layer it is found, the predominantly two-dimensional vortices, that is the inertial convection, transport heat much more efficient than those flow structures that are at large scales more three-dimensional and irregular.

References

[1] H. Hoffmann, D. Weinberg, W. Baumann, K. Hain, W. Leiling, K. Marten, H. Ohira, G. Schnetgöke, K. Thomauske, Scaled model studies of decay heat removal by natural convection for the European fast reactor, Proc. Sixth Int. Topical Meeting on Nuclear Reactor Thermal Hydraulics, Oct. 5-8, 1993, Grenoble, France, Vol. 1, pp. 54-62.

[2] H. Ninokata, Advances in computer simulation of fast breeder reactor thermalhydraulics, Proc. Conf. on Supercomputing in Nuclear Applications, Mito, Japan, March 12-16, 1990, pp. 80-85.

[3] J.U. Knebel, L. Krebs, U. Müller, Experimental investigations on the velocity and temperature field in axisymmetric jets of sodium, Ninth symposium on turbulent shear flows, Kyoto, Japan, August 16-18, 1993.

[4] D. Suckow, Experimentelle Untersuchung turbulenter Mischkonvektion im Nachlauf einer beheizten Kugel, Dr. thesis, University Karlsruhe, KfK 5174, 1993.

[5] M. Wörner, G. Grötzbach, Turbulent heat flux balance for natural convection in air and sodium analysed by direct numerical simulations. Fifth Int. Symposium on Refined Flow Modelling and Turbulence Measurements, Sept. 7-10, 1993, Paris, IAHR-Proc. pp. 335 - 342.

[6] M. Wörner, Direkte Simulation turbulenter Rayleigh-Bénard-Konvektion in flüssigem Natrium, Dr. thesis, University Karlsruhe, KfK 5228, 1994.

[7] R. Krishnamurti, Some further studies on the transition to turbulent convection, JFM 60, 1973, pp. 285-303.

[8] F. Heslot, B. Castaing, A. Libchaber, Transition to turbulence in helium gas, Phys. Rev. A36, 1987, pp. 5870-5873.

[9] S. L. Christie, J. A. Domaradzki, Numerical evidence for nonuniversality of the soft/hard turbulence classification for thermal convection, Phys. Fluids A 5, 1993, pp. 412-421.

[10] R.M. Clever, F.H. Busse, Convection at very low Prandtl numbers, Physics of Fluids, A2, 1990, pp. 334-339.
[11] V. Kek, Bénard Konvektion in flüssigen Natriumschichten, Dr. thesis, University Karlsruhe, KfK 4611, 1989.
[12] V. Kek, U. Müller, Low Prandtl number convection in layers heated from below, Int. J. Heat Mass Transfer 36, 1993, pp. 2795-2804.
[13] R.M. Clever, F.H. Busse, Low Prandtl number convection in a layer heated from below, JFM 102, 1981, pp. 61-74.
[14] A. Chiffaudel, S. Fauve, B. Perrin, Viscous and inertial convection at low Prandtl number: Experimental study, Europhysics Letters 4, 1987, pp. 555-560.
[15] G. Grötzbach, M. Wörner, Flow mechanisms and heat transfer in Rayleigh-Bénard-convection at small Prandtl numbers, ERCOFTAC-Workshop on DNS and LES, Guildford, UK., March 27-30, 1994, Proc. by Kluwer, Dordrecht, Ed. P. Voke, L. Kleiser, J.P. Chollet (1994).
[16] G. Grötzbach, Direct numerical and large eddy simulation of turbulent channel flows, Encyclopaedia of Fluid Mechanics, Gulf Publ. Houston, Vol. 6, 1987, pp. 1337-1391.
[17] M. Wörner, G. Grötzbach, Analysis of semi-implicit time integration schemes for direct numerical simulation of turbulent convection in liquid metals, Notes on Numerical Fluid Mechanics, Ed. J.B. Vos, A. Rizzi, I.L. Ryhming, Vol. 35, pp. 542-551, Verlag Vieweg, Braunschweig, 1992.
[18] H. Schmidt, U. Schumann, H. Volkert, Three-dimensional, direct and vectorized elliptic solvers for various boundary conditions, DFVLR-Mitt. 84-15, August 1984.
[19] U. Schumann, Linear stability of finite difference equations for three-dimensional flow problems, J. Comp. Phys. 18, 1975, pp. 465-470.
[20] G. Grötzbach, Spatial resolution requirements for direct numerical simulation of the Rayleigh-Bénard convection, J. Comp. Phys. 49, 1983, pp. 241-264.
[21] G. Grötzbach, Simulation of turbulent flow and heat transfer for selected problems of nuclear thermal-hydraulics, Proc. Conf. on Supercomputing in Nuclear Applications, Mito, Japan, March 12-16, 1990, pp. 29-35.
[22] M. Wörner, G. Grötzbach, Contributions to turbulence modelling of natural convection in liquid metals by direct numerical simulation, Proc. Mathematical Methods and Supercomputing in Nuclear Applications, Karlsruhe, Germany, April 19-23, 1993, Vol. 1, pp. 224-235.
[23] M. Wörner, G. Grötzbach, Analysis of diffusion of turbulent kinetic energy by numerical simulations of natural convection in liquid metals, Proc. Sixth Int. Topical Meeting on Nuclear Reactor Thermal Hydraulics, Oct. 5-8, 1993, Grenoble, France, Vol. 1, pp. 186-193.
[24] G. Grötzbach, M. Wörner, Analysis of flow mechanisms in Rayleigh-Bénard convection at small Prandtl numbers, Proc. Mathematical Methods and Supercomputing in Nuclear Applications, Karlsruhe, Germany, April 19-23, 1993, Vol. 1, pp. 236-247.
[25] C.-H. Moeng, R. Rotuno, Vertical-velocity skewness in the buoyancy-driven boundary layer, J. Atmos. Sc. 47, 1990, pp. 1149-1162.